Peptide Inhibitors Use Two Related Mechanisms To Alter the Apparent Calcium Affinity of the Sarcoplasmic Reticulum Calcium Pump[†]

Michael R. Afara, Catharine A. Trieber, Delaine K. Ceholski, and Howard S. Young*

Department of Biochemistry, University of Alberta, Edmonton, Alberta, Canada T6G 2H7

Received May 12, 2008; Revised Manuscript Received July 14, 2008

ABSTRACT: The primary sequence of phospholamban (PLB) has provided a template for the rational design of peptide inhibitors of the sarcoplasmic reticulum calcium ATPase (SERCA). In the transmembrane domain of PLB, there are few polar residues and only one is essential (Asn^{34}). Using synthetic peptides, we have previously investigated the role of Asn^{34} in the context of simple hydrophobic transmembrane peptides. Herein we propose that the role of Asn in SERCA inhibition is position-sensitive and dependent upon the distribution of hydrophobic residues. To test this hypothesis, we synthesized a series of transmembrane peptides based on a 24 amino acid polyalanine sequence having either an alternating Leu-Ala sequence (Leu_{12}) or Leu residues at the native positions found in PLB (Leu_9). Asn-containing Leu_9 and Leu_{12} peptides were synthesized with a single Asn residue located either one amino acid (N±1) or one turn of the helix (N±4) in either direction from its native position. Co-reconstitution of these peptides with SERCA into proteoliposomes revealed effects on the apparent calcium affinity and cooperativity of SERCA that correlated with the positions of the Asn and Leu residues. The most inhibitory peptides increased the cooperativity of SERCA as indicated by the Hill coefficients, suggesting that calcium-dependent reversibility is an inherent part of the inhibitory mechanism. Kinetic simulations combined with molecular modeling of the interaction between the peptides and SERCA reveal two related mechanisms of inhibition. Peptides that resemble PLB use the same inhibitory mechanism, whereas peptides that are more divergent from PLB alter an additional step in the calcium transport cycle.

Phospholamban (PLB[1]) is a small integral membrane protein that plays a key regulatory role in the contraction−relaxation cycle of heart muscle (*1, 2*). This cycle involves the release and reuptake of sarcoplasmic reticulum (SR) calcium stores, where calcium recovery into the lumen of the SR is accomplished by an ATP-dependent calcium pump (also known as Ca^{2+}-ATPase or SERCA). The contraction−relaxation cycle in heart muscle is dynamic, in large part due to the involvement of PLB. PLB binds to and inhibits SERCA by decreasing its apparent calcium affinity and slowing the E2 to E1 transition of the catalytic cycle (*3*). PLB contains two major domains (*4*), a phosphoregulatory domain (residues 1−30) and an anchoring transmembrane domain (residues 31−52). The cytosolic domain is highly basic with an N-terminal α-helix followed by a largely unstructured region proximal to the membrane (*5*−*8*). This domain has several residues important in regulating PLB inhibitory functions (*9, 10*) including Ser^{16} and Thr^{17}, which are sites for phosphorylation, and several key residues (Lys^{27} and Asn^{30}) that modulate the physical interaction with SERCA (*11*−*13*). The transmembrane domain is α-helical (*5*−*8*) and is responsible for binding to and inhibiting SERCA (*14*). This domain has been shown to possess inhibitory action of its own, in the absence of the cytosolic domain (*14*−*16*). It is very hydrophobic with only four polar residues: one essential Asn residue and three nonessential Cys residues. The remaining hydrophobic residues line two distinct faces of the transmembrane helix, one that interacts with SERCA and another that participates in a coiled-coil interaction to form homopentamers (*17, 18*). Current models support the idea that the PLB pentamer is an inactive storage form and the PLB monomer is the inhibitory form (*18*−*20*).

There are several detailed molecular models available that describe the regulatory interaction between PLB and SERCA (*8, 21, 22*). These models are based on mutagenesis data (*9, 13, 14, 18, 20*), cross-linking constraints (*11, 12, 22, 23*), NMR structures of PLB (*5*−*8*), and X-ray crystal-

[†] This work was supported by grants from the Heart and Stroke Foundation of Alberta, the Canada Foundation for Innovation, and the Alberta Science and Research Investments Program. H.S.Y. is a Senior Scholar of the Alberta Heritage Foundation for Medical Research. M.R.A. is supported by the Canadian Institutes of Health Research Strategic Training Initiative in Membrane Proteins and Cardiovascular Disease.

* To whom correspondence should be addressed. Phone: 780-492-3931. Fax: 780-492-0886. E-mail: hyoung@ualberta.ca.

[1] Abbreviations: $C_{12}E_8$, octaethylene glycol monododecyl ether; EYPA, egg yolk phosphatidic acid; EYPC, egg yolk phosphatidylcholine; K_{Ca}, calcium concentration at half-maximal activity; n_H, Hill coefficient; PLB, phospholamban; SR, sarcoplasmic reticulum; SERCA, sarco(endo)plasmic reticulum calcium ATPase; V_{max}, maximal activity; Leu_9, acetyl-K_2-LAALAAAAALALAALLLAAAAAALL-K_2-amide; Leu_9N, acetyl-K_2-LAALAANAALALAALLLAAAAAALL-K_2-amide; Leu_9N-1, acetyl-K_2-LAALANAALALAALLLAAAAAALL-K_2-amide; Leu_9N+1, acetyl-K_2-LAALAAANALALAALLLAAAAAALL-K_2-amide; Leu_9N-4, acetyl-K_2-LANLAAAAALALAALLLAAAAAALL-K_2-amide; Leu_9N+4, acetyl-K_2-LAALAAAAALNLAALLLAAAAAALL-K_2-amide; Leu_{10}, acetyl-K_2-LAALAALAALALAALLLAAAAAALL-K_2-amide; Leu_{12}, acetyl-K_2-LALALALALALALALALALALA-K_2-amide; $Leu_{12}N$, acetyl-K_2-LALALNLALALALALALALALA-K_2-amide; $Leu_{12}N-1$, acetyl-K_2-LALANALALALALALALALALA-K_2-amide; $Leu_{12}N-4$, acetyl-K_2-LNLALALALALALALALALALA-K_2-amide; $Leu_{12}N+4$, acetyl-K_2-LALALALALNLALALALALALALA-K_2-amide.

10.1021/bi800880q CCC: $40.75
Published on Web 08/15/2008

lographic structures of SERCA (*24, 25*). The molecular models help to explain the interactions made by the eight essential residues in the transmembrane domain of PLB (Leu[31], Asn[34], Phe[35], Ile[38], Leu[42], Ile[48], Val[49] and Leu[52]), which result in loss of inhibitory function when mutated to Ala (*18*). Of the loss-of-function mutants, the Asn[34] to Ala (N34A) mutation is perhaps the most detrimental to the inhibitory capacity of PLB (*18, 26*). Canine PLB contains three Asn residues (Asn[27], Asn[30] and Asn[34]) that are implicated in the inhibitory interactions with SERCA. While mutation of Asn[27] (Lys[27] in humans) and Asn[30] to Ala greatly enhanced PLB inhibitory action, mutation of Asn[34] to Ala resulted in a complete loss of inhibitory action (*13, 26*). One fundamental question is whether the well-characterized gain-of-function and loss-of-function mutations are context dependent (*16*); i.e., do other interactions involving the highly conserved amino acid sequence of PLB influence the apparent behavior of single point mutations? This concept is supported in the literature, although there have been few such studies. First, double mutants of PLB were constructed by combining gain-of-function mutations with loss-of-function mutations and their effects on inhibition of SERCA were examined (*13*). The double mutant N27A/N34A resulted in a slight recovery of inhibition compared to the N34A loss-of-function mutation alone. In contrast, two other double mutants, N27A/L31A and N30A/L31A, resulted in no significant recovery of inhibition compared to the L31A loss-of-function mutation alone. Second, in a previous study of peptide inhibitors of SERCA (*16*), we took a more extreme approach to this problem. A transmembrane peptide, Leu_9, was synthesized that contained only the nine Leu residues naturally found in PLB, with all other residues substituted with Ala. This peptide retained slight inhibitory activity toward SERCA. Surprisingly, when this same peptide was synthesized with the addition of Asn[34] (Leu_9N, referred to as Asn_1Leu_9 in ref *16*), we obtained a very potent superinhibitor of SERCA. These findings could not have been predicted based on the current understanding of the SERCA-PLB inhibitory interaction.

There have been several studies emphasizing the importance of Asn residues in the thermodynamic stability of transmembrane helices, as well as their association or oligomerization (*27, 28*). Neutral, polar residues such as Asn occur at a low frequency in transmembrane helices, yet they can play a vital functional role (*27, 29*). In the case of PLB, Asn[34] is involved in helix association with SERCA, but it does not seem to influence helix association in the PLB pentamer (*18*). In our previous study of model peptides, we found that a partial requirement for SERCA inhibition is met by a simple hydrophobic surface on a canonical transmembrane α-helix (*16*). The addition of Asn[34] to one of these peptides resulted in superinhibition of SERCA, presumably due to enhanced helix association and hydrogen bonding of Asn[34] of PLB with Thr[317] or Thr[805] of SERCA. In the present study, we systematically varied the position of Asn in two hydrophobic peptides, Leu_9 and Leu_{12} (Figure 1A), and examined the effects of these peptides on SERCA in co-reconstituted proteoliposomes. The apparent calcium affinity and cooperativity of SERCA were dependent upon the distribution of hydrophobic residues, as well as the position of Asn within the transmembrane peptide sequence. Molecular modeling of the SERCA−peptide interaction offers insight into the mechanistic requirements for SERCA inhibition.

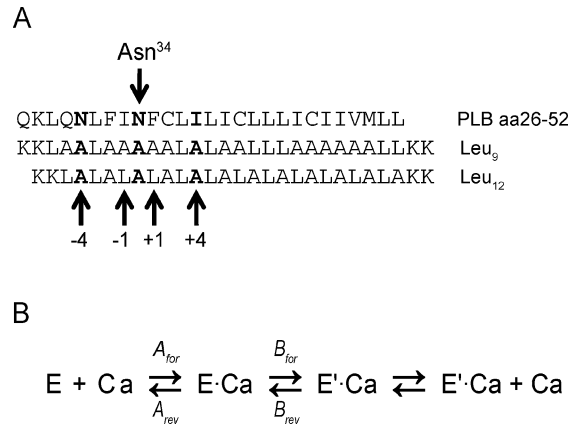

FIGURE 1: (A) Sequence alignment of the Leu_9 and Leu_{12} peptides used in this study, compared to the transmembrane domain of PLB (amino acid residues 26−52). Arrows indicate Asn[34] and the locations chosen for Asn in the synthetic peptides. (B) The reaction scheme and rate constants used as the kinetic model for the initial steps in calcium binding by SERCA.

EXPERIMENTAL PROCEDURES

Materials. Octaethylene glycol monododecyl ether, $C_{12}E_8$, was obtained from Barnet Products (Englewood Cliff, NJ). SM-2 Biobeads were obtained from Bio-Rad (Hercules, CA). Egg yolk phosphatidylcholine (EYPC) and egg yolk phosphatidic acid (EYPA) were obtained from Avanti Polar Lipids (Alabaster, AL). All the reagents used in the coupled enzyme assay (*30*) for measuring Ca^{2+}-dependent ATPase activity were of highest purity available (Sigma-Aldrich, Oakville, ON).

Peptide Synthesis and Purification. Peptide synthesis was carried out by the Alberta Peptide Institute (API, University of Alberta). This procedure has been previously described (*16, 31*). Pure peptide fractions were pooled and lyophilized, and the purified product was evaluated by MALDI-TOF mass spectrometry (Voyager DE Pro, Applied Biosystems, Foster City, CA) and quantitated by amino acid analysis. The following peptides were synthesized (Figure 1A): Leu_9, Leu_9N, Leu_9N-1, Leu_9N+1, Leu_9N-4, Leu_9N+4, Leu_{10} (Leu_9 with a Leu substituted for Asn[34]), Leu_{12}, $Leu_{12}N$, $Leu_{12}N-1$, $Leu_{12}N-4$, $Leu_{12}N+4$. A $Leu_{12}N+1$ peptide was not included in this study because it could not be purified to homogeneity following peptide synthesis. Leu_9N was referred to as Asn_1Leu_9 in ref *16*. Circular dichroism (CD) spectroscopy was performed on the peptides in lipid vesicles as previously described (*16*).

Co-Reconstitution of SERCA and Synthetic Peptides. Skeletal muscle SR vesicles were prepared from rabbit hind leg (*32*) followed by detergent solubilization and purification by Reactive-Red affinity chromatography (*33*). Functional co-reconstitution of SERCA in the presence or absence of synthetic peptides has been previously described (*16, 34*). Briefly, 45 μg of synthetic peptide were resuspended in 100 μL of buffer (20 mM imidazole, pH 7.0, 0.02% NaN_3) and incubated for 15 min at 37°*C* to hydrate. Detergent (700 μg of $C_{12}E_8$) was added followed by vigorous vortexing to solubilize the peptide. EYPC (315 μg) and EYPA (35 μg)

were dried to a thin film under nitrogen gas and lyophilized. The solubilized PLB was added to the lipid film followed by vigorous vortexing to solubilize the lipids. To this suspension of peptide and lipid was added detergent-solubilized, affinity-purified SERCA (305 μg). The final volume was adjusted to 300 μL, and the concentrations were adjusted such that the final molar ratios were 1 SERCA:5 peptides:120 lipids. The detergent was removed by incremental addition of wet SM-2 Biobeads (19 mg) over a 4 h time course at room temperature. The co-reconstituted proteoliposomes containing SERCA and peptide were purified on a sucrose step-gradient (*34*). The molar ratios of peptide-to-SERCA were determined by quantitative SDS−PAGE as previously described (*16, 26*), the lipid concentration was determined by a phosphomolybdate assay (*35, 36*), and the protein concentration was determined by a modified Lowry assay (*37*).

Calcium-Dependent ATPase Activity Measurements. Calcium-dependent ATPase activity of the co-reconstituted vesicles was measured by a coupled-enzyme assay (*30*). All co-reconstituted proteoliposomes in the presence of peptides (SERCA + peptide) were compared to controls in the absence of peptides (SERCA alone), and each assay was performed multiple times using independent co-reconstitutions ($n = 3-5$ for peptide-containing samples; $n = 44$ for matched SERCA controls) over a range of free calcium concentrations from 0.1−10 μM (*16, 26*). Data were plotted as ATPase specific activity (V) versus calcium concentration (μM). The K_{Ca} (calcium concentration at half-maximal activity), the V_{max} (maximal activity) and the n_H (Hill coefficient) were calculated based on nonlinear least-squares fitting of the activity data to the Hill equation using Sigma Plot software (SPSS Inc., Chicago, IL). Errors shown are the standard error of the mean for a minimum of three independent measurements. Statistical comparison of K_{Ca} and n_H parameters was carried out using one-way analysis of variance (between-subjects) followed by Tukey's HSD post hoc test for pairwise comparisons. In all cases, control samples were as follows: (i) negative controls, SERCA reconstituted in the absence of peptide, and SERCA reconstituted in the presence of a noninhibitory peptide (see Leu_{18} in reference (*16*)); and (ii) positive control, SERCA co-reconstituted in the presence of PLB.

Kinetic Simulation. A detailed reaction scheme and rate constants have been described for the transport cycle of SERCA in the absence and presence of PLB (*3*), and we have previously used this model to analyze the effects of synthetic peptide inhibitors on SERCA (*16*). Briefly, we performed a global nonlinear regression fit of the model (*3*) to the SERCA activity curve in the absence and presence of peptides obtained over a range of calcium concentrations (0.1−10 μM) using the software Dynafit (Biokin Inc., Pullman, WA (*38*)). For our reconstituted SERCA proteoliposomes, the equilibrium constant for the binding of the first calcium ion was determined to be 3×10^5 s^{-1} ($A_{forward}$; Figure 1B), which was slightly lower than the initially reported value (*3*). As in our previous work, SERCA activities in the presence of peptides were easily fit with modifications to the rate constants for the slow transitions following calcium binding ($A_{forward}$, $A_{reverse}$, $B_{forward}$ and $B_{reverse}$).

Molecular Modeling. Molecular modeling of the SERCA−peptide interaction was based on the structure of PLB determined by solid-state NMR and docked to SERCA using a flexible protein−protein docking simulation (*8*). We included only the transmembrane domain of PLB (Figure 1A), and the side chains were systematically modified using the program Xfit (*39*) to match the Leu_9N and $Leu_{12}N$ peptides. These SERCA−peptide complexes were then used as templates for understanding the interaction of additional peptides.

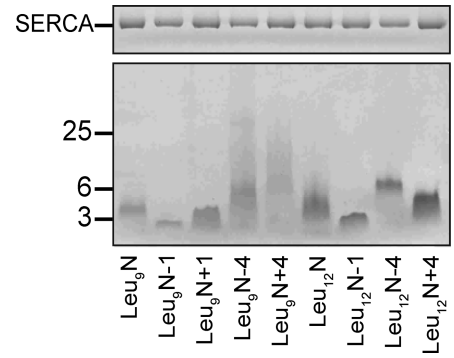

FIGURE 2: Coomassie-stained SDS−PAGE of co-reconstituted proteoliposomes containing SERCA and peptides. Equal amounts of co-reconstituted proteoliposomes were run on 10% (top) and 16% (bottom) polyacrylamide gels (for a subset of the peptides utilized in the study). Molecular mass markers are indicated in kilodaltons; SERCA has a molecular weight of 110 kDa.

RESULTS

Co-Reconstitution of SERCA and Synthetic Peptides. The reconstitution behavior of SERCA has been very well characterized, and has provided a useful system for the study of SERCA inhibition (*16, 26, 40−42*). In our hands, measurement of ATP hydrolysis rates by reconstituted SERCA proteoliposomes typically yielded a K_{Ca} of 0.39 μM Ca^{2+} and a V_{max} of 4.3 ± 0.3 μmol mg^{-1} min^{-1} ($n = 44$). The activity of these proteoliposomes was consistent with previous observations (*16, 26*) and served as one of the negative controls for all further studies in the presence of peptides. In the presence of PLB (*26*), we have previously shown a K_{Ca} of 0.76 μM Ca^{2+} and a V_{max} of 7.4 ± 0.1 μmol mg^{-1} min^{-1} ($n = 10$). To verify that the co-reconstitution of SERCA with the synthetic peptides was comparable to our previous studies (*16, 26*), we examined the efficiency of reconstitution for all peptides in terms of the peptide-to-SERCA and lipid-to-protein molar ratios (data not shown). A typical gel used for quantitative SDS−PAGE is shown in Figure 2. After co-reconstitution and sucrose-gradient purification, the proteoliposomes contained a lipid-to-protein molar ratio of approximately 120-to-1 and a peptide-to-SERCA molar ratio of approximately 4.5-to-1. The peptides may orient randomly in the membrane, but at this ratio of peptide to SERCA there should be two to three peptide molecules correctly oriented to interact with SERCA.

Based on SDS−PAGE and Tricine-SDS−PAGE of our co-reconstituted proteoliposomes, the peptides differ substantially from one another in their migration and staining, despite relatively modest differences in amino acid sequence. This does not reflect peptide quality, since the peptides have been evaluated by MALDI-TOF mass spectrometry following reverse-phase HPLC purification. It is probably due to the small size and extreme hydrophobicity of the peptides

we are studying. For comparison, the gel shown (Figure 2) contains equivalent amounts of loaded protein. Most peptides appear to be primarily monomeric, though small amounts of dimer and trimer are often observed. The presence of peptide oligomers is somewhat variable depending on reconstitution and SDS−PAGE conditions. Despite the prevalence of oligomeric species for PLB, SERCA inhibition is known to saturate at an equimolar stoichiometry of PLB to SERCA (*16, 43, 44*). For all peptides studied, the inhibition of SERCA was maximal at 1 mole of peptide per mole of SERCA, similar to previous observations (*16, 43, 44*).

Lastly, we analyzed the secondary structure of the peptides by CD spectroscopy (data not shown). As with our previous peptides (*16*), the spectra were similar to one another and were consistent with a high α-helical content (minima at 208 and 222 nm). We concluded that Asn insertion had no effect on the α-helical propensity of the peptides in lipid vesicles.

Asn-Containing Leu$_9$ and Leu$_{12}$ Peptides. We systematically inserted Asn into different locations of two previously characterized model peptides, Leu$_9$ and Leu$_{12}$ (*16*). Leu$_9$ has all of the Leu residues naturally found in the transmembrane domain of PLB, with all other residues substituted with Ala. Unlike Leu$_9$, Leu$_{12}$ is a repeating Leu-Ala sequence with the twelve Leu residues arranged around the entire circumference of the peptide. Leu$_{12}$ has been used as a model for the hydrophobic transmembrane segment of an integral membrane protein (*31, 45*), and we have shown that it inhibits SERCA to the same extent as PLB (*16*). Our previous study showed that Leu$_9$ is a weak inhibitor of SERCA, and the addition of the essential Asn^{34} residue created a superinhibitory peptide (Leu$_9$N). Here, we aimed to test the effects of Asn insertion on inhibition by Leu$_9$ and Leu$_{12}$. Twelve peptides were synthesized (Figure 1A): Leu$_9$, Leu$_{12}$, Leu$_9$N, Leu$_{12}$N, Leu$_9$N−1, Leu$_{12}$N−1, Leu$_9$N+1, Leu$_9$N−4, Leu$_{12}$N−4, Leu$_9$N+4, Leu$_{12}$N+4, and Leu$_{10}$ (Leu substituted for Asn^{34}). The peptide nomenclature refers to the relative position of Asn^{34}, where Leu$_9$N−1 refers to an Asn position one amino acid closer to the N-terminus of the peptide. In addition, all of the sequences were capped with two lysine residues at both the N- and C-termini to anchor the peptides across the lipid bilayer.

The Effects of Asn-Containing Peptides on K_{Ca} of SERCA. We tested the ability of these peptides to alter the K_{Ca} of SERCA in co-reconstituted proteoliposomes (Figures 3 and 4A, Table 1). Compared to SERCA alone, the Leu$_9$ peptide was shown to alter the apparent calcium affinity to a lesser extent than PLB (K_{Ca} values of 0.39, 0.55, and 0.76 μM Ca^{2+}, respectively). Inclusion of Asn^{34} in the Leu$_9$ peptide (Leu$_9$N) altered the calcium affinity of SERCA to a much greater extent than PLB (K_{Ca} of 1.17 μM Ca^{2+} versus 0.76 μM Ca^{2+}). In contrast, the Leu$_{12}$ peptide was shown to alter the calcium affinity of SERCA to a similar extent as PLB (K_{Ca} of 0.79 μM Ca^{2+}), and the insertion of Asn^{34} had only a marginal effect on inhibitory action (Leu$_{12}$N; K_{Ca} of 0.85 μM Ca^{2+}).

These findings led us to investigate other amino acid arrangements by varying the position of the Asn residue in the Leu$_9$ and Leu$_{12}$ peptides. Three peptides contained an Asn residue shifted by one amino acid (N±1 peptides), and four peptides contained an Asn residue shifted by four amino acids or one turn of an α-helix (N±4 peptides). As a group, the N±1 peptides (Leu$_9$N−1, Leu$_9$N+1, and Leu$_{12}$N−1) altered the calcium affinity of SERCA to a lesser extent than

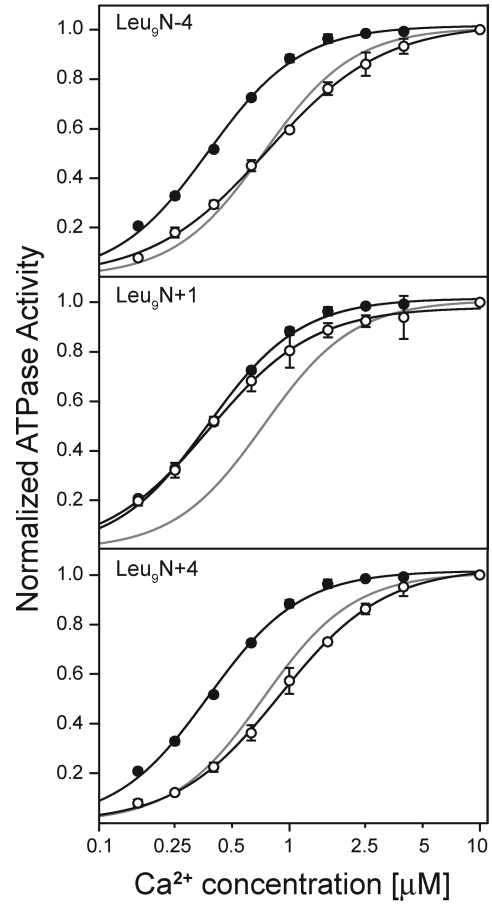

FIGURE 3: Calcium-dependent ATPase activity as a function of free calcium concentration for SERCA co-reconstituted in the absence (●) and in the presence (○) of synthetic peptide inhibitors. The data are shown for the Leu$_9$N−4 (top panel), Leu$_9$N+1 (middle panel), and Leu$_9$N+4 (bottom panel) peptides. For the remaining peptides, refer to Table 1. The data are plotted as normalized ATPase specific activity (V/V_{max}) versus calcium concentration and each data point is the mean ± SEM ($n = 44$ for (●), $n = 3-5$ for (○)). Comparable data are shown for PLB (gray line).

their Leu$_9$N or Leu$_{12}$N counterparts (Table 1). For instance, the apparent calcium affinity of SERCA in the presence of either Leu$_9$N−1 (0.54 μM Ca^{2+}) or Leu$_9$N+1 (0.38 μM Ca^{2+}) was significantly higher than that observed in the presence of Leu$_9$N (1.17 μM Ca^{2+}), indicative of dramatic loss in peptide inhibition. In contrast, shifting the position of the Asn residue by four amino acids resulted in better preservation of inhibitory capacity. As a group, the N±4 peptides (Leu$_9$N−4, Leu$_9$N+4, Leu$_{12}$N−4, and Leu$_{12}$N+4) altered the calcium affinity of SERCA to a similar extent as their Leu$_9$N or Leu$_{12}$N counterparts (Table 1). For instance, the apparent calcium affinity of SERCA in the presence of either Leu$_{12}$N−4 (0.63 μM Ca^{2+}) or Leu$_{12}$N+4 (0.66 μM Ca^{2+}) was similar to that observed in the presence of Leu$_{12}$N (0.85 μM Ca^{2+}), indicative of significant retention of peptide inhibition. In terms of the observed K_{Ca} values, the Leu$_9$N, Leu$_{12}$N, and the N±4 peptides had a high statistical probability of being distinct from SERCA in the absence of peptides ($p < 10^{-2}$). Based on these observations, we conclude that the peptide inhibitors exhibit a clear preference for an Asn residue on one particular face of the transmembrane helix. Like PLB, maximum inhibition occurred when the Asn residue occupied its natural position (Leu$_9$N and Leu$_{12}$N). Unlike PLB, which requires an Asn at position 34,

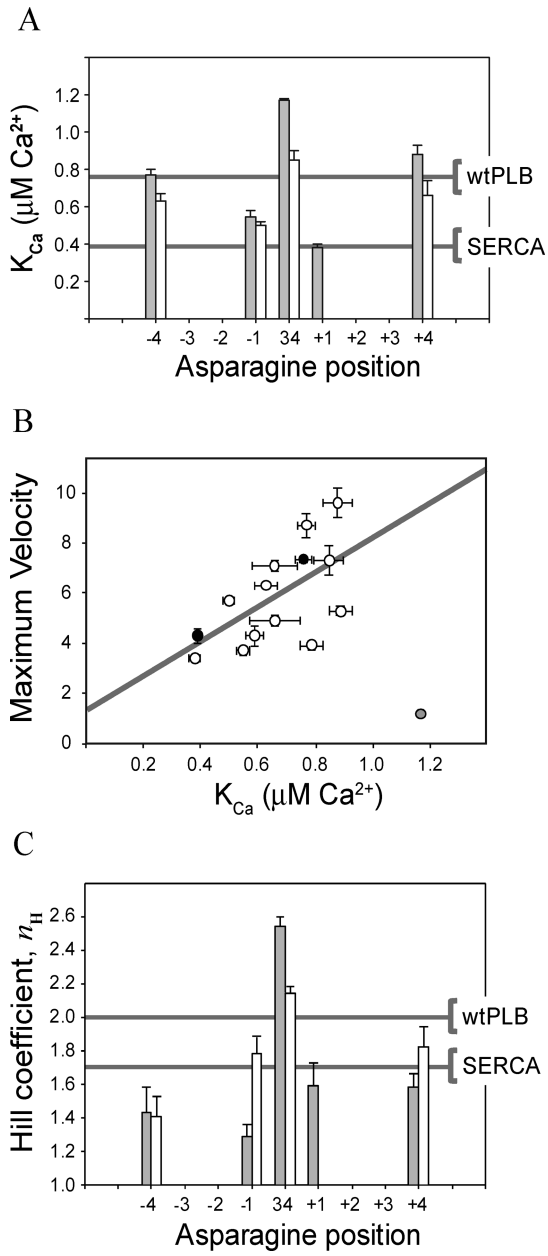

FIGURE 4: Effect of Asn-containing peptides on the apparent calcium affinity (K_{Ca}), maximal velocity (V_{max}) and cooperativity (n_H) of SERCA. (A) The K_{Ca} values are plotted as a function of Asn position for the Leu_9 (gray bars) and the Leu_{12} (white bars) series of peptides. The values for PLB and SERCA and for SERCA alone are indicated. (B) For all peptides, the V_{max} is plotted versus K_{Ca}. Corresponding values for SERCA in the absence and presence of PLB are shown (●). An approximate linear relationship was observed, with Leu_9N being the sole outlier (gray filled circle). (C) The n_H values are plotted as a function of Asn position for the Leu_9 (gray bars) and the Leu_{12} (white bars) series of peptides. The values for PLB and SERCA and for SERCA alone are indicated.

the peptides retained inhibitory function when Asn was located one full helical turn before or after the native Asn^{34} position (Leu_9N-4, Leu_9N+4, $Leu_{12}N-4$, and $Leu_{12}N+4$).

The Effects of Asn-Containing Peptides on V_{max} of SERCA. Our previous studies with co-reconstituted proteoliposomes indicated that PLB and some synthetic peptides increase the maximal activity of SERCA (*16, 26*). To evaluate this behavior for the current set of peptides, we measured their ability to alter the V_{max} of SERCA (Table 1). The V_{max} value

Table 1: Summary of the Data for Peptide Inhibitors of SERCA

co-reconstituted proteoliposomes	K_{Ca} (μM)[a]	V_{max}[b]	n_H[c]
SERCA	0.39 ± 0.01	4.3 ± 0.3	1.7 ± 0.02
PLB_{wt}	0.76 ± 0.03	7.4 ± 0.1	2.0 ± 0.05
Leu_9	0.55 ± 0.02	3.7 ± 0.2	2.1 ± 0.1
Leu_{10}	0.89 ± 0.04	5.3 ± 0.2	1.4 ± 0.1
Leu_{12}	0.79 ± 0.04	3.9 ± 0.2	1.8 ± 0.05
Leu_9N	1.17 ± 0.01	1.2 ± 0.1	2.5 ± 0.06
$Leu_{12}N$	0.85 ± 0.05	7.3 ± 0.6	2.1 ± 0.04
N±1 peptides			
Leu_9N-1	0.54 ± 0.08	3.8 ± 0.5	1.3 ± 0.1
Leu_9N+1	0.38 ± 0.02	3.4 ± 0.1	1.6 ± 0.1
$Leu_{12}N-1$	0.48 ± 0.02	4.5 ± 0.5	1.8 ± 0.1
N±4 peptides			
Leu_9N-4	0.77 ± 0.03	8.7 ± 0.5	1.4 ± 0.1
Leu_9N+4	0.88 ± 0.05	9.6 ± 0.6	1.6 ± 0.08
$Leu_{12}N-4$	0.63 ± 0.04	6.3 ± 0.1	1.4 ± 0.1
$Leu_{12}N+4$	0.66 ± 0.08	7.1 ± 0.2	1.8 ± 0.1

[a] K_{Ca} is the calcium concentration at half-maximal ATPase activity. [b] V_{max} is the maximum velocity attained (μmol mg^{-1} min^{-1}). [c] Hill coefficient.

for SERCA in reconstituted proteoliposomes in the absence of peptides was 4.3 ± 0.3 μmol mg^{-1} min^{-1} (*16, 26*). The V_{max} values for SERCA co-reconstituted in the presence of peptides ranged from 1.2 to 9.6 μmol mg^{-1} min^{-1}. As reported previously for PLB (*26*), a correlation exists between the ability of the peptides to decrease K_{Ca} and to increase V_{max} of SERCA (Figure 4B). For the peptides described herein, plotting K_{Ca} versus V_{max} yielded a reasonable fit to a line ($r = 0.61$). At one end of the scale, the Leu_9N+1 peptide had K_{Ca} and V_{max} values that were similar to SERCA. At the other end of the scale, the Leu_9N+4 peptide had K_{Ca} and V_{max} values higher than PLB. This is a consistent observation with PLB mutants and the peptide inhibitors that remains unexplained. Of course, the Leu_9N peptide deviates from this behavior, which suggests that there is something unique in the regulatory interaction of this peptide with SERCA.

The Effects of Asn-Containing Peptides on Cooperativity of SERCA. The Hill coefficient, n_H, is a measure of the degree of cooperative ligand binding as a function of ligand concentration. Our SERCA activity plots in the absence and presence of peptides (Figure 3) were easily fit to the Hill equation. In good agreement with previous observations, the apparent n_H for SERCA reconstituted in the absence of PLB was 1.7 (*46*), while SERCA co-reconstituted with PLB yielded a value of 2.0 (*9*). This enhancement of SERCA cooperativity reflected in the Hill coefficients is one of the characteristics of PLB inhibition. Three peptides, Leu_9, Leu_9N and $Leu_{12}N$, mimicked this behavior by significantly enhancing SERCA cooperativity as evidenced by the increase in n_H (values of 2.1, 2.5, and 2.1, respectively; Figure 4C and Table 1). This is what we expect from a peptide that mimics PLB. In contrast, the remaining peptides yielded n_H values in the range of 1.4 to 1.8 for SERCA. This reflects a level of cooperativity equivalent to or less than that observed for SERCA in the absence of peptides ($n_H = 1.7$). It was somewhat surprising that the N±4 peptides (Leu_9N-4, Leu_9N+4, $Leu_{12}N-4$, and $Leu_{12}N+4$) were effective inhibitors of SERCA (Figure 4A), yet they failed to enhance cooperativity (Figure 4C). This suggests that proper positioning of an Asn residue in the interaction with SERCA was a

more stringent requirement for enhancement of cooperativity than it was for inhibition. Moreover, this was true for both arrangements of hydrophobic residues (Leu_9 and Leu_{12}), confirming our earlier observation that a simple hydrophobic surface meets a partial requirement for SERCA inhibition (*16*).

The Effects of the Leu_{10} Peptide on SERCA. Given that the Leu_{12} peptide inhibits SERCA at a level comparable to that observed for PLB, we hypothesized that Leu may substitute for Asn in the functional interaction with SERCA. This idea contradicts recent molecular models (*8, 21, 22*) that are consistent with hydrogen bond formation between Asn^{34} of PLB and Thr^{317} and/or Thr^{805} of SERCA as a major determinant of inhibition. To test this hypothesis, we synthesized a Leu_{10} peptide that contained the nine naturally occurring Leu residues of PLB, as well as a tenth Leu residue located at position 34. Compared to SERCA alone, the Leu_{10} peptide altered the apparent calcium affinity to a similar extent as PLB (K_{Ca} values of 0.39, 0.89, and 0.76 μM Ca^{2+}, respectively; Table 1), indicating that hydrogen bond formation by Asn is not required to lower the apparent calcium affinity of SERCA. However, the observed Hill coefficient ($n_H = 1.4 \pm 0.1$) indicated that the Leu_{10} peptide did not enhance cooperativity as observed for PLB and the Leu_9, Leu_9N and $Leu_{12}N$ peptides. These findings suggest a link between the proper positioning of an Asn residue and the increase in cooperativity associated with SERCA inhibition.

Reaction Rate Constant Simulations. In an attempt to explain the link between the calcium affinity and cooperativity experimentally observed for SERCA inhibition, we utilized kinetic simulation of our ATPase activity curves (*3*). The kinetic model assumes that the binding of calcium to SERCA occurs as two highly cooperative, sequential events linked by a conformational transition (Figure 1B). It is postulated that the calcium transport cycle of SERCA has a slow structural transition ($E\cdot Ca \leftrightarrow E'\cdot Ca$), which increases the affinity of the enzyme for a second calcium, thereby accounting for the activation and cooperativity of SERCA. PLB primarily alters the rate constant for an isomeric transition following binding of the first calcium ion ($B_{reverse}$), resulting in the increase in cooperativity and the shift in calcium affinity observed experimentally (*3, 16*). For the peptides, the experimentally observed changes in the cooperativity and calcium affinity could be explained by altering the magnitude of the forward and reverse rate constants for the first two steps in calcium binding: (i) step A, corresponding to binding of the first calcium ion ($E + Ca \leftrightarrow E\cdot Ca$); and (ii) step B, corresponding to a conformational change following calcium binding ($E\cdot Ca \leftrightarrow E'\cdot Ca$). This analysis revealed that the peptides could be grouped according to their effects on the Hill coefficient and cooperativity of SERCA (Table 2). In the first group of inhibitory peptides (Leu_9N-4, Leu_9N+4, $Leu_{12}N-4$, $Leu_{12}N+4$, and Leu_{10}), the Hill coefficients were unchanged compared to SERCA in the absence of peptides. The reverse rate constants for steps A and B increase and drive the reaction toward the calcium-free state ($E + Ca$). The primary sequences of these peptides were more divergent from PLB. In the second group of inhibitory peptides (Leu_9, Leu_9N, and $Leu_{12}N$), the Hill coefficients were increased compared to SERCA in the absence of peptides. In this case, only the reverse rate constant for step B increases, which allows binding of the first calcium ion ($E\cdot Ca$) but prevents the conformational change following calcium binding ($E'\cdot Ca$). The primary sequences of these peptides more closely resembled PLB. The net result is that group 1 peptides have a low $A_{forward}/A_{reverse}$ ratio and a low n_H favoring the dissociation of calcium, while group 2 peptides have a high $A_{forward}/A_{reverse}$ ratio and a high n_H favoring binding of the first calcium ion (Figure 1B). This latter behavior is characteristic of PLB and requires optimal surface complementarity and/or a properly positioned Asn residue in the peptide inhibitor.

Table 2: Summary of the Kinetic Simulations in the Absence and Presence of Peptides

		reaction rate constants (s^{-1})			
	n_H	$A_{forward}$	$A_{reverse}$	$B_{forward}$	$B_{reverse}$
SERCA alone	1.7 ± 0.02	3×10^5	0.001	30	57
group 1 peptides[a]	1.6 ± 0.1	4×10^5	3×10^4	51	1×10^6
group 2 peptides[b]	2.2 ± 0.1	3×10^5	0.001	32	2×10^6

[a] Group 1 peptides included Leu_9N-4, Leu_9N+4, $Leu_{12}N-4$, $Leu_{12}N+4$, Leu_{10}. [b] Group 2 peptides included Leu_9, Leu_9N, and $Leu_{12}N$.

DISCUSSION

PLB and several leucine-containing polyalanine peptides are comparable inhibitors of SERCA (*16*). This has led us to propose that a simple hydrophobic surface in a transmembrane α-helix meets a partial requirement for SERCA inhibition (*16*). Herein, we wished to further address this hypothesis by examining two transmembrane peptides (Leu_9 and Leu_{12}) and the mechanistic role of Leu and Asn residues in inhibition. The Leu_9 peptide is based on the amino acid sequence of PLB, and as expected it retains weak inhibitory capacity. The Leu_{12} peptide contains an alternating $(Leu-Ala)_{12}$ sequence that has been well studied as a model hydrophobic transmembrane helix (*31, 45*). This Leu_{12} peptide has a very different distribution of Leu residues than is found in PLB, yet it possesses comparable inhibitory capacity. This is suitably explained by recent molecular models of the interaction between PLB and SERCA (Figure 5) (*8, 21*). In comparison to PLB, the alternating Leu-Ala sequence satisfies several criteria for interaction with SERCA: (i) no steric clashes are created by the distribution of Leu and Ala residues; (ii) interactions at either end of the peptide helix are maintained, particularly with Trp^{932} and Phe^{92} of SERCA; and (iii) additional hydrophobic contacts are created that help to stabilize the association with SERCA along the C-terminal half of the peptide helix (potential SERCA interaction sites include Phe^{92}, Trp^{794}, Leu^{797}, Val^{798}, Ile^{956}, and Phe^{957}).

In the context of the Leu_9 and Leu_{12} hydrophobic peptides described above, we examined the mechanistic role of Asn in the functional interaction with SERCA. Asn^{34} is the only essential polar amino acid in the transmembrane domain of PLB, and it has been implicated in forming a hydrogen bond with Thr^{317} and/or Thr^{805} of SERCA (*16, 21*). We hypothesized that our Asn-containing peptide inhibitors share this feature of SERCA inhibition. If this is correct, SERCA inhibition should be very sensitive to moving the Asn residue to a different face of the transmembrane helix (±1 amino acid position) or by one complete turn of the helix (±4 amino acid positions). Our results show that peptides with Asn

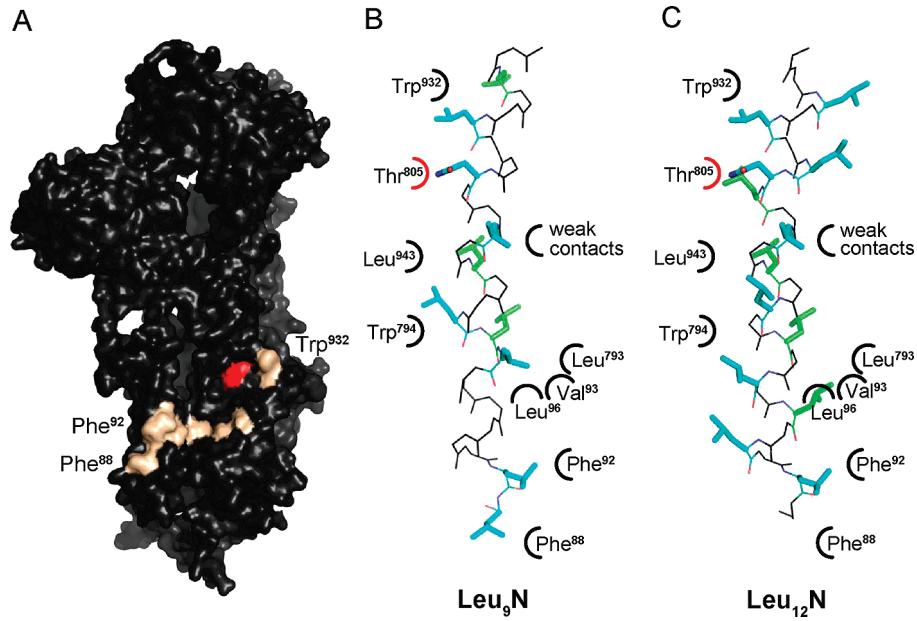

FIGURE 5: Potential interactions between the E2 form of SERCA (pdb accession code 2AGV) and the Leu_9N and $Leu_{12}N$ peptides. (A) Surface representation of SERCA with potential interaction sites shown including Phe^{88}, Phe^{92}, Val^{93}, Leu^{96}, Leu^{793}, Trp^{794}, Trp^{932}, and Leu^{943}. The proposed interaction site of PLB Asn^{34} (Thr^{805} of SERCA) is indicated as a red surface. (B, C) Ligand plots comparing the interactions of Leu_9N and $Leu_{12}N$ with potential sites on SERCA. Peptide side chains that face the lipid bilayer are colored green. The interaction with Thr^{805} is highlighted in red.

positioned in the native location exhibit the typical inhibitory behavior of PLB, including reduced calcium affinity and enhanced cooperativity of cation binding to SERCA. Moving the Asn residue one helical turn before or after the native position resulted in significant inhibition of SERCA (greater than 50% of the inhibition seen in the presence of Leu_9N or $Leu_{12}N$), yet the enhancement of cooperativity was not observed. Not surprisingly, moving the Asn residue one amino acid before or after the native position resulted in significant loss of inhibitory capacity (less than 50% of the inhibition seen in the presence of Leu_9N or $Leu_{12}N$). Finally, substituting a Leu residue for Asn in the Leu_9N peptide (Leu_{10}) also resulted in significant inhibition of SERCA with no enhancement of cooperativity. Taken together, these results link the correct positioning of an Asn residue with both the reduction in calcium affinity and enhancement of cooperativity observed for PLB inhibition.

SERCA inhibition by PLB is a dynamic process that depends on many factors, including the cytosolic calcium concentration (*47*), and the phosphorylation (*46*) and aggregation states (*18*) of PLB. SERCA inhibition by PLB is maximal at low calcium concentrations (~0.1 μM) and absent at high calcium concentrations (~10 μM). One of the hallmarks of PLB inhibition is the rapid recovery of SERCA function over a relatively narrow range of calcium concentrations (calcium-dependent reversal of inhibition). The data presented support a mechanistic model in which the effects of peptide inhibitors on the calcium affinity and cooperativity of SERCA can be separated into distinct modes of interaction. In the first mode of binding, a simple hydrophobic surface is sufficient to alter the apparent calcium affinity of SERCA. In a second mode of binding, surface complementarity and/or hydrogen bonding between a properly positioned Asn residue and Thr^{317}/Thr^{805} of SERCA narrows the range of calcium concentrations over which SERCA activity recovers (i.e., enhances cooperativity). Asn residues rarely occur in hydrophobic transmembrane helices, but when present, they often play a vital role in protein−protein interactions. One such role is transmembrane helix association (*27*), as is the case between the transmembrane domain of PLB and one or more transmembrane helices of SERCA. We can then understand the mechanism of calcium-mediated recovery of SERCA activity as the unlocking of complementary surfaces and the breaking of a hydrogen bond in the association of transmembrane helices. Moreover, this process appears to be directly responsible for the enhancement of cooperative calcium binding by SERCA. A hydrophobic surface is necessary and sufficient for lowering the apparent calcium affinity of SERCA, while surface complementarity and/or hydrogen bond formation decrease the sensitivity of SERCA to calcium at low concentrations and enhance the sensitivity to calcium at high concentrations (Figure 6).

In the well-characterized reaction scheme for calcium transport by SERCA (*3*), a slow structural transition follows binding of the first of two calcium ions to SERCA. The kinetic model assumes that the binding of calcium to SERCA occurs as two highly cooperative, sequential events interspaced by a conformational transition (Figure 1B). It is postulated that binding of the first calcium ion induces a slow structural transition ($E{\cdot}Ca \leftrightarrow E'{\cdot}Ca$) that activates SERCA and increases the affinity of the enzyme for binding of a second calcium ion. The reverse rate constant ($B_{reverse}$) for this reaction step increases in the presence of PLB, resulting in the shift in calcium affinity observed experimentally. Using Dynafit software (*38*), we simulated our activity curves (ATP hydrolysis versus calcium concentration) in the absence and presence of peptides. The results identify particular steps in the calcium transport cycle of SERCA that are associated with inhibition by the peptides. In the first mode of peptide binding, the interaction of hydrophobic surfaces shifts the calcium affinity of SERCA, and this is completely explained by large increases in $A_{reverse}$ and $B_{reverse}$, the rate constants for the reverse transition ($E + Ca \leftarrow E{\cdot}Ca \leftarrow E'{\cdot}Ca$). In

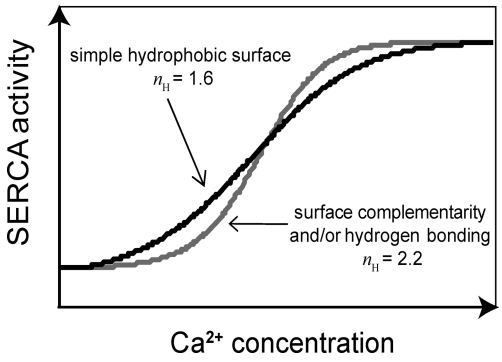

FIGURE 6: The effects of peptide−SERCA interactions on the calcium-dependence of SERCA activity. Group 1 peptides interact with SERCA primarily through a simple hydrophobic surface involving van der Waals interactions. These peptides have little effect on the cooperative calcium binding mechanism of SERCA (n_H = 1.6). Group 2 peptides interact with SERCA through a combination of surface complementarity and polar (potential hydrogen bonding) interactions (n_H = 2.2). These peptides markedly enhance the cooperative calcium binding mechanism of SERCA. Group 1 peptides included Leu_9N-4, Leu_9N+4, $Leu_{12}N-4$, $Leu_{12}N+4$, Leu_{10}. Group 2 peptides included Leu_9, Leu_9N, and $Leu_{12}N$.

the second mode of peptide binding, enhanced surface complementarity and/or hydrogen bonding increase the cooperativity of SERCA, and this is completely explained by a large increase in $B_{reverse}$ with no effect on $A_{reverse}$. The net effect is that binding of the first calcium ion is favored ($E + Ca \rightarrow E{\cdot}Ca$), but the slow isomeric transition required for binding of the second calcium ion is suppressed ($E{\cdot}Ca \leftarrow E'{\cdot}Ca$).

ACKNOWLEDGMENT

We thank Dr. Robert Parker of API for the peptide synthesis.

REFERENCES

1. Kirchberger, M., Tada, M., and Katz, A. (1975) Phospholamban: a regulatory protein of the cardiac sarcoplasmic reticulum. *Recent Adv. Stud. Cardiac Struct. Metab. 5*, 103–115.
2. Katz, A. M., Repke, D. I., Kirchberger, M. A., and Tada, M. (1974) Calcium-binding sites and calcium uptake in cardiac microsomes: effects of varying Ca^{2+} concentration, and of an adenosine-3′,5′-monophosphate-dependent protein kinase. *Recent Adv. Stud. Cardiac Struct. Metab. 4*, 427–436.
3. Cantilina, T., Sagara, Y., Inesi, G., and Jones, L. R. (1993) Comparative studies of cardiac and skeletal sarcoplasmic reticulum ATPases: effect of phospholamban antibody on enzyme activation. *J. Biol. Chem. 268*, 17018–17025.
4. Simmerman, H. K. B., Collins, J. H., Theibert, J. L., Wegener, A. D., and Jones, L. R. (1986) Sequence analysis of phospholamban: identification of phosphorylation sites and two major structural domains. *J. Biol. Chem. 261*, 13333–13341.
5. Lamberth, S., Schmid, H., Muenchbach, M., Vorherr, T., Krebs, J., Carafoli, E., and Griesinger, C. (2000) NMR solution structure of phospholamban. *Helv. Chim. Acta 83*, 2141–2152.
6. Zamoon, J., Mascioni, A., Thomas, D. D., and Veglia, G. (2003) NMR solution structure and topological orientation of monomeric phospholamban in dodecylphosphocholine micelles. *Biophys. J. 85*, 2589–2598.
7. Oxenoid, K., and Chou, J. (2005) The structure of phospholamban pentamer reveals a channel-like architecture in membranes. *Proc. Natl. Acad. Sci. U.S.A. 102*, 10870–10875.
8. Seidel, K., Andronesi, O. C., Krebs, J., Griesinger, C., Young, H. S., Becker, S., and Baldus, M. (2008) Structural characterization of Ca^{2+}-ATPase-bound phospholamban in lipid bilayers by solid-state nuclear magnetic resonance (NMR) spectroscopy. *Biochemistry 47*, 4369–4376.
9. Toyofuku, T., Kurzydlowski, K., Tada, M., and MacLennan, D. H. (1994) Amino acids Glu^2 to Ile^{18} in the cytoplasmic domain of phospholamban are essential for functional association with the Ca^{2+}-ATPase of sarcoplasmic reticulum. *J. Biol. Chem. 269*, 3088–3094.
10. Sharma, P., Patchell, V. B., Gao, Y., Evans, J. S., and Levine, B. A. (2001) Cytoplasmic interactions between phospholamban residues 1−20 and the calcium-activated ATPase of the sarcoplasmic reticulum. *Biochem. J. 355*, 699–706.
11. Jones, L. R., Cornea, R. L., and Chen, Z. (2002) Close proximity between residue 30 of phospholamban and cysteine 318 of the cardiac Ca^{2+} pump revealed by intermolecular thiol cross-linking. *J. Biol. Chem. 277*, 28319–28329.
12. Chen, Z., Stokes, D. L., Rice, W. J., and Jones, L. R. (2003) Spatial and dynamic interactions between phospholamban and the canine cardiac Ca^{2+} pump revealed with use of heterobifunctional cross-linking agents. *J. Biol. Chem. 278*, 48348–48356.
13. Kimura, Y., Asahi, M., Kurzydlowski, K., Tada, M., and MacLennan, D. H. (1998) Phospholamban domain Ib mutations influence functional interactions with the Ca^{2+}-ATPase isoform of cardiac sarcoplasmic reticulum. *J. Biol. Chem. 273*, 14238–14241.
14. Kimura, Y., Kurzydlowski, K., Tada, M., and MacLennan, D. H. (1996) Phospholamban regulates the Ca^{2+}-ATPase through intramembrane interactions. *J. Biol. Chem. 271*, 21726–21731.
15. Karim, C. B., Marquardt, C. G., Stamm, J. D., Barany, B., and Thomas, D. D. (2000) Synthetic null-cysteine phospholamban analogue and the corresponding transmembrane domain inhibit the Ca-ATPase. *Biochemistry 39*, 10892–10897.
16. Afara, M., Trieber, C., Glaves, J., and Young, H. (2006) Rational design of peptide inhibitors of the sarcoplasmic reticulum calcium pump. *Biochemistry 45*, 8617–8627.
17. Simmerman, H. K. B., Kobayashi, Y. M., Autry, J. M., and Jones, L. R. (1996) A leucine zipper stabilizes the pentameric membrane domain of phospholamban and forms a coiled-coil pore structure. *J. Biol. Chem. 271*, 5941–5946.
18. Kimura, Y., Kurzydlowski, K., Tada, M., and MacLennan, D. H. (1997) Phospholamban inhibitory function is enhanced by depolymerization. *J. Biol. Chem. 272*, 15061–15064.
19. Autry, J. M., and Jones, L. R. (1997) Functional co-expression of the canine cardiac Ca^{2+} pump and phospholamban in *Spodoptera frugiperda* (Sf21) cells reveals new insights on ATPase regulation. *J. Biol. Chem. 272*, 15872–15880.
20. Cornea, R. L., Autry, J. M., Chen, Z., and Jones, L. R. (2000) Re-examination of the role of the leucine/isoleucine zipper residues of phospholamban in inhibition of the Ca^{2+}-pump of cardiac sarcoplasmic reticulum. *J. Biol. Chem. 275*, 41487–41494.
21. Toyoshima, C., Asahi, M., Sugita, Y., Khanna, R., Tsuda, T., and MacLennan, D. H. (2003) Modeling of the inhibitory interaction of phospholamban with the Ca^{2+} ATPase. *Proc. Natl. Acad. Sci. U.S.A. 100*, 467–472.
22. Chen, Z., Akin, B. L., Stokes, D. L., and Jones, L. R. (2006) Cross-linking of C-terminal residues of phospholamban to the Ca^{2+} pump of cardiac sarcoplasmic reticulum to probe spatial and functional interactions within the transmembrane domain. *J. Biol. Chem. 281*, 14163–14172.
23. Chen, Z., Stokes, D. L., and Jones, L. R. (2005) Role of leucine 31 of phospholamban in structural and functional interactions with the Ca^{2+} pump of cardiac sarcoplasmic reticulum. *J. Biol. Chem. 280*, 10530–10539.
24. Obara, K., Miyashita, N., Xu, C., Toyoshima, I., Sugita, Y., Inesi, G., and Toyoshima, C. (2005) Structural role of countertransport revealed in Ca^{2+} pump crystal structure in the absence of Ca^{2+}. *Proc. Natl. Acad. Sci. U.S.A. 102*, 14489–14496.
25. Toyoshima, C., and Nomura, H. (2002) Structural changes in the calcium pump accompanying the dissociation of calcium. *Nature 418*, 605–611.
26. Trieber, C. A., Douglas, J., Afara, M., and Young, H. S. (2005) The effects of mutation on the regulatory properties of phospholamban in co-reconstituted membranes. *Biochemistry 44*, 3289–3297.
27. Choma, C., Gratkowski, H., Lear, J. D., and DeGrado, W. F. (2000) Asparagine-mediated self-association of a model transmembrane helix. *Nat. Struct. Biol. 7*, 161–166.
28. Zhou, F. X., Merianos, H. J., Brunger, A. T., and Engelman, D. M. (2001) Polar residues drive association of polyleucine transmembrane helices. *Proc. Natl. Acad. Sci. U.S.A. 98*, 2250–2255.
29. Goldstein, J., Lehnhardt, S., and Inouye, M. (1991) In vivo effect of asparagine in the hydrophobic region of the signal sequence. *J. Biol. Chem. 266*, 14413–14417.

30. Warren, G. B., Toon, P. A., Birdsall, N. J. M., Lee, A. G., and Metcalfe, J. C. (1974) Reconstitution of a calcium pump using defined membrane components. *Proc. Natl. Acad. Sci. U.S.A. 71*, 622–626.
31. Zhang, Y. P., Lewis, R. N., Henry, G. D., Sykes, B. D., Hodges, R. S., and McElhaney, R. N. (1995) Peptide models of helical hydrophobic transmembrane segments of membrane proteins. 1. Studies of the conformation, intrabilayer orientation, and amide hydrogen exchangeability of Ac-K_2-$(LA)_{12}$-K_2-amide. *Biochemistry 34*, 2348–2361.
32. Eletr, S., and Inesi, G. (1972) Phospholipid orientation in sarcoplasmic reticulum membranes: spin-label ESR and proton NMR studies. *Biochim. Biophys. Acta 282*, 174–179.
33. Stokes, D. L., and Green, N. M. (1990) Three-dimensional crystals of Ca-ATPase from sarcoplasmic reticulum: symmetry and molecular packing. *Biophys. J. 57*, 1–14.
34. Young, H. S., Rigaud, J. L., Lacapere, J. J., Reddy, L. G., and Stokes, D. L. (1997) How to make tubular crystals by reconstitution of detergent-solubilized Ca^{2+}-ATPase. *Biophys. J. 72*, 2545–2558.
35. Chen, P. S., Toribara, T. Y., and Warner, H. (1956) Microdetermination of phosphorous. *Anal. Chem. 28*, 1756–1758.
36. Chester, D. W., Herbette, L. G., Mason, R. P., Joslyn, A. F., and Triggle, D. J. (1987) Diffusion of dihydropyridine calcium channel antagonists in cardiac sarcolemmal lipid multibilayers. *Biophys. J. 52*, 1021–1030.
37. Markwell, M. H., Hass, S. M., Beiber, L. L., and Tolbert, N. E. (1978) A modification of the Lowry procedure to simplify protein determination in membrane and lipoprotein samples. *Anal. Biochem. 87*, 206–210.
38. Kuzmic, P. (1996) Program DYNAFIT for the analysis of enzyme kinetic data: application to HIV Proteinase. *Anal. Biochem. 237*, 260–273.
39. McRee, D. E. (1999) XtalView/Xfit-A versatile program for manipulating atomic coordinates and electron density. *J. Struct. Biol. 125*, 156–165.
40. Stokes, D. L., Pomfret, A. J., Rice, W. J., Glaves, J. P., and Young, H. S. (2006) Interactions between Ca^{2+}-ATPase and the pentameric form of phospholamban in two-dimensional co-crystals. *Biophys.l J. 90*, 4213–4223.
41. Levy, D., Gulik, A., Bluzat, A., and Rigaud, J.-L. (1992) Reconstitution of the sarcoplasmic reticulum Ca^{2+}-ATPase: mechanisms of membrane protein insertion into liposomes during reconstitution procedures involving detergents. *Biochim. Biophys. Acta 1107*, 283–298.
42. Reddy, L. G., Cornea, R. L., Winters, D. L., McKenna, E., and Thomas, D. D. (2003) Defining the molecular components of calcium transport regulation in a reconstituted membrane system. *Biochemistry 42*, 4585–4592.
43. Ferrington, D., Yao, Q., Squier, T., and Bigelow, D. (2002) Comparable levels of Ca-ATPase inhibition by phospholamban in slow-twitch skeletal and cardiac sarcoplasmic reticulum. *Biochemistry 41*, 13289–13296.
44. Waggoner, J., Huffman, J., Griffith, B., Jones, L., and Mahaney, J. (2003) Improved expression and characterization of Ca^{2+}-ATPase and phospholamban in High-Five cells. *Protein Expression Purif. 34*, 56–67.
45. Zhang, Y. P., Lewis, R. N., Hodges, R. S., and McElhaney, R. N. (1995) Peptide models of helical hydrophobic transmembrane segments of membrane proteins. 2. Differential scanning calorimetric and FTIR spectroscopic studies of the interaction of Ac-K_2-$(LA)_{12}$-K_2-amide with phosphatidylcholine bilayers. *Biochemistry 34*, 2362–2371.
46. Antipenko, A. Y., Spielman, A. I., Sassaroli, M., and Kirchberger, M. A. (1997) Comparison of the kinetic effects of phospholamban phosphorylation and anti-phospholamban monoclonal antibody on the calcium pump in purified cardiac sarcoplasmic reticulum membranes. *Biochemistry 36*, 12903–12910.
47. Asahi, M., McKenna, E., Kurzydlowski, K., Tada, M., and MacLennan, D. H. (2000) Physical interactions between phospholamban and sarco(endo)plasmic reticulum Ca^{2+}-ATPases are dissociated by elevated Ca^{2+}, but not by phospholamban phosphorylation, vanadate, or thapsigargin, and are enhanced by ATP. *J. Biol. Chem. 275*, 15034–15038.

BI800880Q